DEVELOPMENT OF MODEL FOR PREDICTING THE FLEXIBLE PAVEMENT STRENGTH

Thanapon Thepwong[1,*] and Boonchai Sangpetngam[2]

[1,2] Department of Civil Engineering, Faculty of Engineering, Chulalongkorn University, Bangkok, THAILAND
**Corresponding author; E-mail address: mindchai@hotmail.com*

Abstract

In the present, roads in Thailand are mainly asphalt pavements. While traffic is applying on the road, it is also damaging the pavement structure. Currently the remaining pavement strength can be assessed by pavement surface deflection measurement by using the Falling Weight Deflectometer test. However, knowing the changes of pavement strength over future time is also needed to plan for the pavement rehabilitation works. This research presents the development of pavement strength over time. The objectives are to develop a statistical model between pavement strength and factors affecting asphalt pavement. Then the pavement strength model is compared with the test data of actual asphalt pavement. The factors that affect pavement strength are type of base material, number of standard axle repetition applying on the pavement, temperature, and season.

Keywords: Asphalt pavement, pavement strength, deflection, structural number, prediction model

1. Introduction

In the present, roads in Thailand are mainly asphalt concrete (AC) pavement. While traffic is applying on the road, it is also damaging the pavement structure. Estimation of remaining pavement strength can be assessed by using the Falling Weight Deflectometer (FWD) test. This machine test can get output data such as surface deflection which is indicator for pavement damage to evaluate pavement strength. The output data has used to assign maintenance for pavement for the purpose of increasing pavement life. The deflection from FWD test depends on load, temperature, season, and pavement structure [1,2].

However, knowing the changes of pavement strength over future time is also needed to plan for the pavement rehabilitation works. The design life for AC pavement of Department of Rural Roads (DRR) is 7 years or 10 years [3] and Department of Highways (DOH) which survey pavement damage across the country in the past is 15 years [4]. Thus, this research will simulate pavement strength model from the factors which affect pavement damage for AC pavement. The research objectives are to develop a statistical model between pavement strength and factors affecting asphalt concrete pavement. Then the pavement strength model is compared with the test data of actual asphalt pavement. Research scope selects only AC pavements to use factors which affecting asphalt concrete pavement and use AC pavement design from DOH. Then compares with scatter plot with deflection or structural number from simulation model and deflection or structural number from FWD test that data has sourced from DOH.

2. Theory and research methodology

2.1 Deflection and pavement strength

Deflection is variable which estimates pavement strength. The deflection test can use nondestructive testing (NDT) which set load into the pavement. The output for NDT test is pavement deflection at testing location or at the center of load. The distance which far away from test location cause a smaller deflection than the deflection at the center of load. When combine these two deflections together, the output for FWD test is deflection basin. the deflection evaluation has advantage such as evaluate remaining pavement strength for all structure, increase efficiency of pavement to support traffic in the future [5], find cause that pavement structure has damaged, and prioritize maintenance for rehabilitation [1]. The factors which affect pavement deflection are type of pavement structure, load, temperature, and season [1,2]. NDT of FWD test use impact loading. DOH test and evaluate with FWD load at 754 kPa which is similar as 25 tons truck and load location test at rutted by wheel of vehicle [6].

Modulus is a variable which relate to pavement strength. This research set modulus to resilient modulus. When pavement has been received load repetitions, it will cause permanent deformation [7].

2.2 Traffic prediction

Traffic is the important factor for affecting road damaged and increase deflection. the main factors for traffic are truck traffic and type of truck [7,8]. The equation for calculating total equivalent single axle load (ESAL) shown in Eq. (1). The ESAL prediction relates with growth factor as shown in Eq. (2). The equation for evaluating growth factor is shown in Eq. (3).

$$Total\ ESAL = \sum ESAL_i \quad (1)$$

$$ESAL_i = ADT_0 \times T_i \times (T_f)_i \times G \times D \times L \times 365 \quad (2)$$

$$G = \frac{(1+g)^n - 1}{g} \quad (3)$$

$ESAL_i$ = Equivalent single axle load of type i truck
ADT_0 = Average daily traffic (Vehicles/day)
T_i = Percentage of type i truck in decimal
$T_{f,i}$ = Truck factor of type i truck
L = Percentage of lane distribution in decimal
D = Percentage of directional distribution in decimal
G = Growth factor
g = Percentage of growth rate in decimal
n = Total year for design

Lane distribution from each road depend on traffic and total lane as shown in Table 1. Truck factors for each vehicle are from weigh station in Thailand as shown in Table 2.

Table 1 Truck distribution for multiple-lane-controlled access highways [9].

One-way ADT	Outer lane distribution		One-way ADT	Outer lane distribution	
	2 lanes	3 or more lanes		2 lanes	3 or more lanes
2000	94	82	30000	72	59
4000	88	76	35000	70	58
6000	85	72	40000	69	57
8000	82	70	50000	67	55
10000	81	68	60000	66	53
15000	77	65	70000	-	52
20000	75	63	80000	-	51
25000	73	61	100000	-	49

Table 2 Truck factor for each truck [10].

One-way ADT	Truck factor (DOH year 2009)
2 Axles Truck	1.03
3-4 Axles Truck	1.57
Semi-Trailer	2.93
Trailer	5.90

2.3 Structural number

Structural number (SN) is variable relevant for pavement strength. It depends on thickness, type of material, and drainage coefficient for each layer in pavement structures [8]. The equation for evaluating total SN is shown in Eq. (4).

$$SN = a_1 D_1 + a_2 D_2 m_2 + a_3 D_3 m_3 \quad (4)$$

a_i = Layer coefficient in ith layer
D_i = Thickness in ith Layer (in)
m_i = Drainage coefficient in ith layer

Pavement layer coefficient depend on type of material by evaluating from layer modulus which developed from AASHTO 1986 design guide [11] as shown in Eq. (5).

$$a_i = a_g \left(\frac{E_i}{E_g} \right)^{\frac{1}{3}} \quad (5)$$

a_g = Layer coefficient of standard material as listed in
E_i = Layer resilient modulus
E_g = Resilient modulus of standard material as listed in Table 3

Table 3 Layer coefficient and resilient modulus of standard material in AASHO road test [11].

Layer type	Layer coefficient (a_g)	Resilient modulus (E_g) (MPa)
Asphalt concrete surface coarse	0.44	3100
Untreated and stabilized base coarse	0.14	207
Granular subbase coarse	0.11	104

2.4 Backcalculation

Backcalculation is pavement strength evaluation by using a deflection from FWD test. The factors which affect SN from backcalculation are deflection, load, and pavement structure [8]. Backcalculation evaluates from Eq. (6), Eq. (7), and Eq. (8).

$$Design\ M_R = CM_R = C\left(\frac{0.24P}{d_r r} \right) \quad (6)$$

$$d_0 = 1.5pa\left\{\frac{1}{M_R\sqrt{1+\left(\frac{D}{a}\sqrt[3]{\frac{E_p}{M_R}}\right)^2}} + \frac{\left[1-\frac{1}{\sqrt{1+\left(\frac{D}{a}\right)^2}}\right]}{E_p}\right\} \quad (7)$$

$$SN_{eff} = 0.0045D\sqrt[3]{E_p} \quad (8)$$

Design M_R = Design subgrade resilient modulus (psi)

M_R = Backcalculated subgrade resilient modulus (psi)

P = FWD applied load (lb)

C = Adjustment factor = 0.33

d_r = Deflection at r distance from the center of load (in)

r = Distance from center of load (in)

d_0 = FWD deflection at the center of the load plate (in)

p = FWD applied pressure (psi)

a = Plate radius (in)

D = Total thickness of all pavement layer above the subgrade (in)

E_p = Effective Modulus of pavement layer above the subgrade (psi)

Distance from center of load (r) can use deflection at 36 in from center of load. The comparison with backcalculation from FWD test and laboratory resilient modulus test are reasonably well [12].

2.5 Remaining life

The main factors for affecting pavement in Thailand are 2 types such as fatigue damage and rutting damage [4]. The damage for AC pavement and cement-treated base (CTB) is fatigue damage. The CTB is bound material and base material mix with cement material. The damage for unbound materials is rutting damage. Remaining life for each layer can be evaluated by mechanistic empirical design guide (MEPDG). Fatigue life for AC depends on asphalt mixture, AC thickness, and strain from pavement response and fatigue life for CTB depends on pavement response and type of CTB which depend on modulus of rupture (MR) [13,14]. Evaluation of AC life is shown in Eq. (9). This equation depends on AC mix as shown in Eq. (10) and type of cracking as shown in Eq. (11) and Eq. (12). Evaluation of CTB life is shown in Eq. (13).

$$N_{f-HMA} = k_{f1}(C)(C_H)\beta_{f1}(\varepsilon_t)^{k_{f2}\beta_{f2}}(E_{HMA})^{k_{f3}\beta_{f3}} \quad (9)$$

$$C = 10^{4.84\left(\frac{V_{be}}{V_a+V_{be}}-0.69\right)} \quad (10)$$

For bottom-up or alligator cracking

$$C_H = \frac{1}{0.000398 + \frac{0.003602}{1+e^{(11.02-3.49H_{HMA})}}} \quad (11)$$

For top-down or longitudinal cracking

$$C_H = \frac{1}{0.01 + \frac{12.00}{1+e^{(15.676-2.8186H_{HMA})}}} \quad (12)$$

$$\log(N_{f-CTB}) = \frac{0.972\beta_{c1} - \left(\frac{\sigma_t}{MR}\right)}{0.0825\beta_{c2}} \quad (13)$$

N_f = Number of repetitions to fatigue cracking (ESAL)

ε_t = Tensile strain at critical locations and calculated by the structural response model

E_{HMA} = Dynamic modulus of the asphalt concrete measured in compression (psi)

k_{f1}, k_{f2}, k_{f3}= Global field calibration parameters (k_{f1}=0.007566, k_{f2}= -3.9492, k_{f3}= -1.281)

β_{f1}, β_{f2}, β_{f3}= Local or mixture specific field calibration constants (Global calibration were set to 1.0)

V_{be} = Effective asphalt content by volume (%)

V_a = Air void in asphalt concrete mixture (%)

C_H = Thickness correction term, dependent on type of cracking

H = Total asphalt concrete thickness (in)

σ_t = Tensile stress at the bottom of the CTB layer (psi)

MR = 28-day modulus of rupture for the CTB layer (psi)

β_{c1}, β_{c2}= Local calibration constants (Global were set to 1.0)

The rutting life of unbound material has general equation which depend on developer as shown in Eq. (14).

$$N_r = a\varepsilon_v^{-b} \quad (14)$$

N_r = Number of repetitions to rutting (ESAL)

ε_v = Compression strain at critical locations and calculated by the structural response model

a, b = Material constants shown as Table 4

Table 4 Rutting criteria and material constants by various developer [7].

Developer	Maximum rutting (in)	a	b
Asphalt Institute	0.5	1.365×10^{-9}	-4.477
Shell	0.5	1.94×10^{-7}	-4
Transport Research Laboratory	0.4	6.18×10^{-8}	-3.95

2.6 Mechanistic empirical pavement design guide

Simulation with MEPDG is developed from AASHTO pavement design guide. This section is divided to AC material, unbound material and CTB material.

2.2.1 AC material

Factors for AC Material design are pavement temperature, asphalt mixture, gradation of rock, time of loading, and air voids. The equation for evaluation is Dynamic Modulus (E*) which depend on temperature and binder viscosity. Evaluation for AC Material is level 2 [14] as shown in Eq. (15), Eq. (16), and Eq. (17).

$$\log(E^*) = \delta + \frac{\alpha}{1+e^{\beta+\gamma \log t_r}} \quad (15)$$

$$\log(t_r) = \log(t) - c\left(\log(\eta) - \log(\eta_{t_r})\right) \quad (16)$$

$$\log\log\eta = A + VTS\log T_R \quad (17)$$

E^* = Dynamic modulus (psi)
t = Time of loading (s)
t_r = Time of loading at the reference temperature (s)
δ = Minimum Value of E^*
$\delta+\alpha$ = Maximum Value of E^*
β,γ = Parameter describing shape of sigmoidal function
γ = 0.313351
c = 1.255882
η = Binder viscosity (cP)
T_R = Temperature (Rankine)
A = Regression Intercept
VTS = Regression slope of viscosity temperature susceptibility

Asphalt aging is the main factor for affecting AC Modulus. It depends on asphalt material by used original binder viscosity and AC hardness. Evaluation for binder viscosity at mix-lay down as shown in Eq. (18) which depends on AC hardness as shown in Eq. (19) and Eq. (20).

$$\log\log(\eta_{t=0}) = a_0 + a_1 \log\log(\eta_{orig}) \quad (18)$$

$$a_0 = 0.054405 + 0.004082 \times code \quad (19)$$

$$a_1 = 0.972035 + 0.010886 \times code \quad (20)$$

$\eta_{t=0}$ = Mix/lay down viscosity (cP)
η_{orig} = Original viscosity (cP)
code = hardening ratio (0 for average)

The next step is aging viscosity evaluation by using mix-lay down viscosity and time after mix-lay down as shown in Eq. (21). Each parameter relates with using mix-lay down viscosity, asphalt temperature, air temperature, binder viscosity at reference temperature as shown in Eq. (22), Eq. (23), Eq. (24), and Eq. (25). The adjustment for aging viscosity is shown in Eq. (26). This equation depends on air voids, time, air temperature and AC viscosity as shown in Eq. (27) and Eq. (28).

$$\log\log(\eta_{aged}) = \frac{\log\log(\eta_{t=0}) + At}{1+Bt} \quad (21)$$

$$A = -0.004166 + 1.41213C + \log MAAT + D\log\log(\eta_{t=0}) \quad (22)$$

$$B = 0.197725 + 0.068384\log C \quad (23)$$

$$C = 10^{274.4946 - 193.831\log T_R + 33.9366\log(T_R)^2} \quad (24)$$

$$D = -14.5521 + 10.47662\log T_R - 1.88161\log(T_R)^2 \quad (25)$$

$$\log\log(\eta_{aged})' = F_v \log\log(\eta_{aged}) \quad (26)$$

$$F_v = \frac{1 + 1.0367\times 10^{-4}(VA)(t)}{1+6.1798\times 10^{-4}(t)} \quad (27)$$

$$VA = \frac{VA_{orig} + 0.011(t) - 2}{1 + 4.24\times 10^{-4}(t)(Maat) + 1.169\times 10^{-3}\left(\frac{t}{\eta_{orig,77}}\right)} + 2 \quad (28)$$

η_{aged} = Aged viscosity (cP)
t = Time of aging asphalt (month)
MAAT = Mean annual air temperature (°F)
T_R = Asphalt temperature (Rankine)
η_{aged}' = Aged viscosity at time t (cP)
VA = Air voids
VA_{orig} = initial air voids
$\eta_{orig,77}$= Original binder vicosity at 77 °F (MPoise)

The next step is aging viscosity at mid-depth evaluation by used mix-lay down viscosity, and depth as shown in Eq. (29). This equation relates with air temperature as shown in Eq. (30).

$$\eta_{t,z} = \frac{\eta_t(4+E) - E(\eta_{t=0})(1-4z)}{4(1+Ez)} \quad (29)$$

$$E = 23.83e^{(-0.0308MAAT)} \quad (30)$$

$\eta_{t,z}$ = Aged viscosity at time t, and depth z (MPoise)
η_t = Aged surface viscosity (MPoise)
z = Depth (in)

The last step is modulus evaluation by time from ESAL and design modulus [5]. The equation is shown in Eq. (31) which relates to AC damage as shown in Eq. (32).

$$E^*_{dam} = 10^\delta + \frac{E^* - 10^\delta}{1 - e^{(-0.3+5\log D)}} \quad (31)$$

$$D = \frac{n}{N_f} \quad (32)$$

E^*_{dam} = Asphalt concrete modulus at damage level of D (psi)

E^* = Undamaged asphalt concrete modulus (psi)

δ = Minimum Value of E^* from master curve

N_f = Number of repetitions to fatigue cracking (ESAL)

D = Damage level in decimal

n = Number of axle-load application at t time (ESAL)

2.2.2 Unbound material

The unbound material resilient modulus depends on stress in each layer from pavement response and moisture content [14]. The equation for determining resilient modulus by time and moisture content is shown in Eq. (33) and Eq. (34). The equation depends on stress as shown in Eq. (35) and Eq. (36).

$$\log\frac{M_R}{M_{Ropt}} = a + \frac{b-a}{1+e^{\left(\ln\left(-\frac{b}{a}\right)+k_s\left(S-S_{opt}\right)\right)}} \quad (33)$$

$$M_{Ropt} = k_1 p_a \left(\frac{\theta}{p_a}\right)^{k_2}\left(\frac{\tau_{oct}}{p_a}\right)^{k_3} \quad (34)$$

$$\theta = \sigma_1 + \sigma_2 + \sigma_3 \quad (35)$$

$$\tau_{oct} = \frac{1}{3}\sqrt{\left(\sigma_1-\sigma_2\right)^2+\left(\sigma_1-\sigma_3\right)^2+\left(\sigma_2-\sigma_3\right)^2} \quad (36)$$

M_R = Unbound material resilient modulus

M_{Ropt} = Unbound material resilient modulus at optimum moisture content

a = Minimum of $\log(M_R/M_{Ropt})$

b = Maximum of $\log(M_R/M_{Ropt})$

k_s = Regression parameter

$S-S_{opt}$ = Variation in degree of saturation in decimal

σ_1 = Major stress

σ_2 = Intermediate stress

σ_3 = Minor stress

Moisture content is the main factor for affecting resilient modulus. If unbound material moisture increase, resilient modulus will decrease. The equation has been developed by adding moisture variable and suitable in Thailand [15] as shown in Eq. (37) for fine material and Eq. (38) for coarse material.

$$M_R(MPa) = 271\left(\frac{\theta}{P_a}\right)^{0.0137}\left(\frac{\tau_{oct}}{P_a}+1\right)^{0.991}(\%w)^{-0.451} \quad (37)$$

$$M_R(MPa) = 252\left(\frac{\theta}{P_a}\right)^{0.086}\left(\frac{\tau_{oct}}{P_a}+1\right)^{1.107}(\%w)^{-0.479} \quad (38)$$

P_a = Atmospheric pressure = 101.3 kPa

%w = Unbound material moisture content

k_s parameter is relevant with plasticity index (PI) of unbound material. The equation develop from MEPDG and suitable for fine-grained soil and non-plastic soil [16] as shown in Eq. (39).

$$k_m = 0.362PI + 3.545 \quad (39)$$

k_m = Regression Parameter = k_s

PI = Plasticity index (%)

2.2.3 CTB material

The CTB Material damage is fatigue. CTB modulus depends on stress at bottom of layer from pavement response, MR and traffic [13,14] as shown in Eq. (40) and Eq. (41).

$$E_{CSM}(t) = E_{CSM}(min) + \frac{E_{CSM}(max) - E_{CSM}(min)}{1-e^{(-4+14D)}} \quad (40)$$

$$D = \frac{n}{N_f} \quad (41)$$

E_{CSM} (t)= CTB Modulus at damage level of D (psi)

E_{CSM} (min)= Minimum CTB modulus (psi)

E_{CSM} (max)= Maximum CTB modulus (psi)

N_f = Number of repetitions to fatigue cracking (ESAL)

D = Damage level in decimal

n = Number of axle-load application at t time (ESAL)

2.7 Change of modulus by shakedown

Change of modulus in each layer depends on load. If layer has taken load continuously, it would have caused shakedown which depends on load state as shown in Fig. 1.

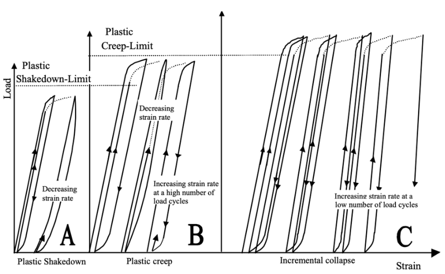

Fig. 1 Behavior of shakedown under repeated cyclic load in unbound materials [17]

Range A – plastic shakedown: applied load is smaller than plastic shakedown limit and the response is plastic only for a finite number of load repetitions but after completion of the post-compaction period, the response becomes entirely resilient, and no further permanent strain occurs.

Range B – plastic creep: applied load is greater than plastic shakedown limit. During the first load cycles, the high level of plastic strain rate decreases for the time being to a low, nearly constant level. The number of load cycles for reaching this constant level of strain rate depends on the material and the load level.

Range C – incremental collapse: applied load is greater than plastic creep limit. The response is always plastic. The permanent strain rate depends on load level and decreases very slowly compared with Range A and B or not at all.

Change of modulus depends on range of shakedown. The unbound modulus in range A and B will not change by traffic and will slightly increase in range C. A moisture at 2% in range C will increase modulus 11% from traffic 2,000 to 10,000 load cycles [18] as shown in Fig. 2.

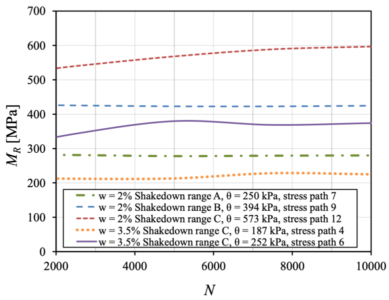

Fig. 2 Evolution of resilient modulus with number of load repetitions for different shakedown range [18]

The shakedown for bitumen-stabilized material with 700 kPa load. Permanent strain will not change from 1 million times traffic [19]. A para rubber AC material by using 200 kPa deviator stress, it found that permanent strain at 0-2000 load cycles [20].

2.8 Change of deflection

Change of deflection by using canterbury accelerated pavement testing indoor facility (CAPTIF) and simulating pavement structure found that deflection at post compaction slightly increase when compare with deflection at 112,000 load cycles and load increment increase deflection and decrease pavement life [21]. The prediction model for change of deflection is shown in Eq. (42).

$$N \geq 5{,}000{,}000 e^{\left(-0.0206 \Delta d_0\right)} \tag{42}$$

N = Average pavement life for 15 mm rutting (ESAs)

Δd_0 = Percentage of change in central deflections during the post-compaction period

When pavement life at 10 percentiles from field compare with pavement life at 50 percentiles from CAPTIF, this comparative is similar. Pavement life from CAPTIF test use for change of deflection prediction model. The model is relevant for change of deflection in range -0.2 to 0.2 mm for CAPTIF test [22]. The equation for change of deflection is shown in Eq. (43), Eq. (44) and Eq. (45).

$$N_d < 5{,}000{,}000 e^{\left(-0.023 \Delta d_0\right)} \tag{43}$$

$$\Delta d_0 = mean\left(\delta d_0\right) + 1.65 standard\ deviation\left(\delta d_0\right) \tag{44}$$

$$\delta d_0 = \frac{d_{0yr1} - d_{0yr0}}{d_{0yr0}} \times 100 \tag{45}$$

N_d = Design traffic life (ESAs)

d_{0yr1} = Central deflection at year 1

d_{0yr0} = Central deflection at year 0

3. Process

3.1 Route selection for comparing with simulation model

Route selection selects only FWD test with same section and various time to simulate. Pavement structure at surface layer is AC pavement, subgrade layer is unbound material, base and sublease layer is unbound material or CTB material. The AC pavement with unbound material selects road No. 2 at chainage 268 to 268.5. AC pavement that base is CTB material selects road No. 344 at chainage 25.8 to 62.6.

3.2 BISAR pavement response simulation program

Shell Research developed BISAR in the early 1970s, which was used in drawing the design charts of Shell Pavement Design Manual issued in 1978. The version Release R 1.0 of BISAR program was issued in 1987 as BISAR-PC. Later, Shell develops BISAR 1.0 to DOS program as BISAR-PC 2.0 in 1995 and BISAR 3.0 for Windows 3.1, Windows 95, and Windows NT [23]. BISAR can simulate pavement response with pavement structure, type of material and thickness. The output data show deflection, stress and strain in specific point in pavement structure.

3.3 Pavement structure simulation and comparison

Simulation starts with modulus design, then simulates pavement response with BISAR program to obtain stress, strain, and deflection in each layer. The AC layer selects critical point at top and bottom of layer. The CTB layer selects critical point at bottom of layer. The unbound layer except subgrade layer selects critical point at mid-depth layer. The subgrade layer selects critical point at top of layer. Design parameters for AC and unbound material use modulus and Poisson ratio as shown in Table 5.

Table 5 Design parameter for simulation in each material [24,25].

Material	Design Modulus (MPa)	Poisson ratio
PMA or AC 40-50	4,500	0.35
AC 60-70	2,500	0.35
Crushed Rock	350	0.35
Subbase	150	0.35
Selected Material	100	0.35
Subgrade	10 x CBR (%)	0.35

Note: CBR = California Bearing Ratio (%)

Design parameters for simulation in CTB material use MR, Modulus, Poisson ratio as shown in Table 6.

Table 6 Design parameter for simulation in CTB material [14].

Material	Design Modulus (psi)	Modulus of rupture (psi)	Poisson ratio
CTB	1,000,000	200	0.20

Note: 145.038 psi = 1 MPa

The next step is simulation for AC pavement. This procedure accumulates with damaged modulus and aging modulus as shown in Eq. (46) and Eq. (47). Aging AC for simulation uses medium mix design which each parameter data refers from NCHRP as shown in Table 7.

$$E_{AC,t} = E_{D,t} + \Delta E_{AG,t} \tag{46}$$

$$\Delta E_{AG,t} = E_{AG,0} + E_{AG,t} \tag{47}$$

$E_{AC,t}$ = Total modulus at time t

$E_{D,t}$ = AC damaged modulus at time t

$E_{AG,0}$ = AC aging modulus after construct at mid-depth

$E_{AG,t}$ = AC aging modulus at time t and mid-depth

Table 7 Design parameter for simulation in aging AC [14].

Parameter	Medium mix Value
Air voids (%)	7
Effective Binder Content (%)	11
A	11.01
VTS	-3.701
δ	2.8234
α	3.9435
β	-0.7920

Aging AC use mean annual air temperature in 2021, mean annual air temperature is 27.5 °C [26], then evaluates mean annual air temperature from 2012 to 2022 in Thailand by using Weather Underground database as shown in Table 8.

Table 8 Design mean annual air temperature for aging AC in Thailand.

Year	Mean annual air temperature (°C)	Year	Mean annual air temperature (°C)
2012	28.19	2017	27.37
2013	27.92	2018	27.00
2014	27.12	2019	27.78
2015	27.71	2020	27.72
2016	27.73	2021	27.50 [26]
2017	27.37	2022	27.24

The next step is simulation for unbound materials. This procedure evaluates by using stress in each layer, optimum water content, specific gravity, unit weight and PI from laboratory. Design parameter is shown in Table 9 and saturation evaluation is shown in Eq. (48).

Table 9 Design parameter for simulation in unbound materials.

Material	Specific gravity	Optimum moisture content (%)	Unit weight (t/m³)	PI (%)
Crushed Rock	2.65 [27]	5.54	2.289	0
Subbase Material	2.85 [28]	7.30	2.084	6.48
Selected Material A	2.85 [28]	9.52	1.918	6.29
Selected Material B	2.66 [28]	4.92	1.966	4.45
Subgrade	2.75 [29]	11.04	2.001	23.78

$$S = \frac{G_S w}{e} = \frac{G_S w}{\frac{G_S \gamma_w}{\gamma_d} - 1} \tag{48}$$

S = Degree of saturation (%)

G_s = Material specific gravity

w = Material water content (%)

e = Void ratio

γ_w = Water density (20 °C : γ_w = 0.9982)

γ_d = Material dry density

The next step is pavement modulus simulation by time. The pavement life selects the minimum pavement life between AC and CTB to simulate traffic in each time. The design life for simulation is 10 years. Then evaluates modulus by time with fatigue damage in MEPDG. The unbound material layers simulate with moisture content which depends on month and environment.

Final step is SN and deflection evaluation by time to compare change of SN and change of deflection with BISAR Program. The field test of FWD load set at the reference load is difficult, so deflection may be error. The deflection can adjust from actual load to reference load [30] as shown in Eq. (49).

$$\text{Normalized deflection} = \text{Actual deflection} \times \frac{\text{Reference load}}{\text{Actual load}} \quad (49)$$

4. Result

4.1 Deflection simulation result and comparison

The simulation set change of unbound modulus by shakedown to unchanged. Simulation for unbound base found that trend line for change of deflection decreases at post-compaction and increases at approximate 40% of pavement life. Change of aging modulus in AC smaller than change of damage modulus at post-compaction. Afterwards, change of aging modulus larger than change of damage modulus. The deflection simulation for unbound base material is shown in Fig. 3.

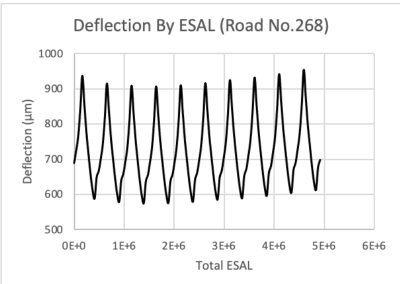

Fig. 3 Deflection pattern for unbound material

The simulation that base is CTB material found that change of deflection slightly decreases trend line at post-compaction. Then, it significantly increases at approximate 20% of pavement life. Finally, it slightly increases or remains unchanged at approximate 70% of pavement life that stage is destroyed. This deflection simulation is shown in Fig. 4.

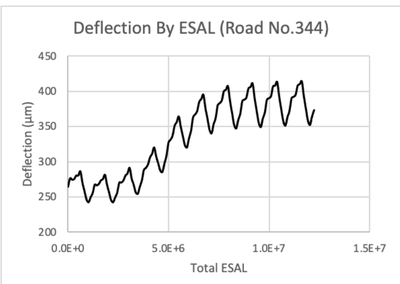

Fig. 4 Deflection pattern for CTB material

Comparison for change of deflection which obtain from FWD test and simulation from BISAR program found that there is good correlation in range -30% to 45%. This range is similar as change of deflection range from Arnold [22] as shown in Fig. 5.

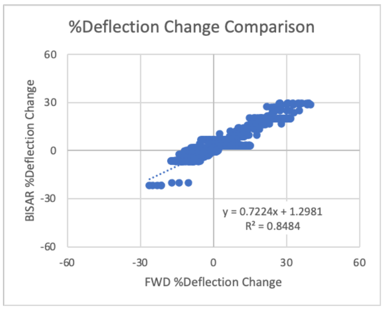

Fig. 5 Change of deflection compare between BISAR and FWD test

4.2 SN simulation result and comparison

The simulation set change of unbound modulus by shakedown to unchanged. Simulation for unbound base found that trend line for change of SN increases at post-compaction and decreases at approximate 30% of pavement life. Change of aging modulus in AC smaller than change of damage modulus at post-compaction. After that, change of aging modulus larger than change of damage modulus. Change of SN is opposite result with change of deflection for unbound base. The SN simulation for unbound base material is shown in Fig. 6.

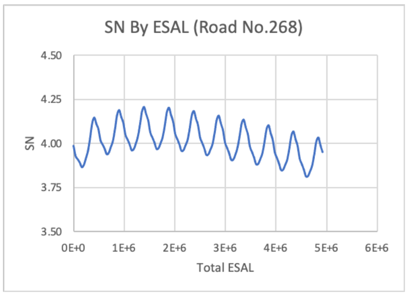

Fig. 6 SN pattern for unbound material

The simulation that base is CTB material found that change of deflection slightly increases trend line. After that, it decreases significantly at approximate 20% of pavement life. Finally, it slightly decreases or remains unchanged at approximate 70% of pavement life that stage is destroyed. Change of SN is opposite result in change of deflection for CTB material. The SN simulation for CTB material is shown in Fig. 7.

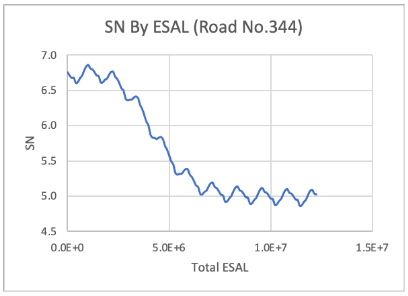

Fig. 7 SN pattern for CTB material

Comparison for change of SN with backcalculation from FWD deflection and SN from simulation model found that there is good correlation in range -15% to 10% as shown in Fig. 8.

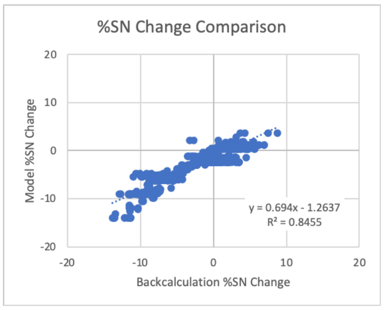

Fig. 8 Change of SN compare between BISAR and backcalculation from FWD test

5. Conclusion

AC Pavement strength depends on ESAL, thickness, layer material, temperature, and season. Pavement damage can evaluate by using FWD to determine damage and remaining pavement strength.

Change of deflection for AC and unbound base slightly decreases trend line at post-compaction. After that, it slightly increases at approximate 30% of pavement life. Change of SN for AC and unbound base slightly increases trend line at post-compaction. Then, it slightly decreases at approximate 30% of pavement life.

Change of deflection for AC and CTB slightly decreases trend line at post-compaction. Then, it significantly increases when traffics apply from approximate 20% to 70% of pavement life. Finally, it slightly decreases or remains unchanged. Change of SN for AC with CTB increases trend line at post-compaction. Then, it significantly decreases when traffics apply from approximate 20% to 70% of pavement life. After that, it slightly decreases or remains unchanged.

Comparison with FWD test and simulation model has good correlation range at -30% to 45% for change of deflection and -15% to 10% for change of SN.

Change of deflection and change of SN can use for predicting pavement strength in each period. DOH and DRR can evaluate pavement strength, predict SN or deflection, and plan for rehabilitation before AC pavement is completely damaged.

Acknowledgement

The author wishes to acknowledge Assoc. Prof. Dr. Boonchai Sangpetngam for being advisor and providing support for this research project, Nutchanon Phantapanichakul, Panupong Yencham, and DOH to import FWD test for evaluation and comparison with simulation model.

Reference

[1] Bureau of Maintenance. (2020, 9 January). Deflection testing with falling weight deflectometer (In Thai). Retrieved 6 July from https://maintenance.drr.go.th/wp-content/uploads/2020/01/drr-2020-01-09_04-12-31_184743.pdf

[2] Smith, K. D., Bruinsma, J. E., Wade, M. J., Chatti, K., Vandenbossche, J. M., & Yu, H. T. (2017). Using Falling Weight Deflectometer Data with Mechanistic-Empirical Design and Analysis, Volume I: Final Report (FHWA-HRT-16-009). Federal Highway Administration.

[3] Bureau of location and design. (2018a). Standard drawing for road design (In Thai).

[4] Svasdisant, T., Anuvechsirikiat, S., Promjaree, N., & Thipthong, C. (2008). Asphalt pavement distresses survey and related causes investigation (In Thai), (RD 261). Bureau of Road Research and Development.

[5] Pierce, L. M., Bruinsma, J. E., Smith, K. D., Wade, M. J., Chatti, K., & Vandenbossche, J. M. (2017). Using Falling Weight Deflectometer Data With Mechanistic-Empirical Design and Analysis, Volume III: Guidelines for Deflection Testing, Analysis, and Interpretation (FHWA-HRT-16-011). Federal Highway Administration.

[6] Sedokbaub, P., Sawangsuriya, A., Pheuakthong, T., & Chukaew, S. (2014). Evaluation study of asphalt concrete pavement structure type for heavy vehicles and high-volume roads (In Thai) (RD 307). Bureau of Road Research and Development.

[7] Huang, Y. H. (2004). Pavement analysis and design. Pearson Education.

[8] AASHTO. (1993). AASHTO guide for design of pavement structures, 1993 (Vol. 1). The Association.

[9] Darter, M. I., Becker, J. M., Snyder, M. B., & Smith, R. E. (1985). PORTLAND CEMENT CONCRETE PAVEMENT EVALUATION SYSTEM (COPES) (NCHRP Report 277).

[10] Logistics and Digital Supply Chain. (2013). Truck weight category study project (In Thai).

[11] Rohde, G. T., & Hartman, A. (1996). COMPARISON OF PROCEDURES TO DETERMINE STRUCTURAL NUMBER FROM FWD DEFLECTIONS. COMBINED 18TH ARRB TRANSPORT RESEARCH CONFERENCE AND TRANSIT NEW ZEALAND LAND TRANSPORT SYMPOSIUM, 2-6 SEPTEMBER 1996, CHRISTCHURCH, NEW ZEALAND PART 4.,

[12] Wu, Z., & Gaspard, K. (2009). Mechanistic flexible pavement overlay design program (FHWA/LA.08/454). Louisiana Transportation Research Center.

[13] AASHTO. (2011). Mechanistic-empirical pavement design guide : a manual of practice. American Association of State Highway and Transportation Officials.

[14] NCHRP 1-37A. (2004). Mechanistic-Empirical Design of New and Rehabilitated Pavement Structures. Transportation Research Board, National Research Council.

[15] Phommavone, C., & Sangpetngam, B. (2018). Influences of Moisture Content on Resilient Modulus of Unbound Crushed Limestone. Engineering Journal, 22, 39-49.

[16] Naji, K. (2018). Resilient modulus–moisture content relationships for pavement engineering applications. International Journal of Pavement Engineering, 19(7), 651-660.

[17] Werkmeister, S., Dawson, A. R., & Wellner, F. (2001). Permanent Deformation Behavior of Granular Materials and the Shakedown Concept. Transportation Research Record, 1757(1), 75-81.

[18] Rahman, M. S., & Erlingsson, S. (2016). Influence of Post Compaction on the Moisture Sensitive Resilient Modulus of Unbound Granular Materials. Procedia Engineering, 143, 929-936.

[19] Puichaisorn, P., & Sangpetngam, B. (2022). Permanent Deformation Behavior under Repeated Load of Recycled Material Stabilized with Bitumen Emulsion. Engineering Journal, 26(4), 13-23.

[20] Silimanotham, H., & Sangpetngam, B. (2020). Effects of crumbed para rubber on permanent deformation resistance of hot mix asphalt. IOP Conference Series: Materials Science and Engineering, 849, 012060.

[21] Werkmeister, S., & Alabaster, D. (2007). Estimation of Remaining Pavement Life of Low-Volume Roads with Falling Weight Deflectometer Results: A Practical Method. Transportation Research Record, 1989-2(1), 261-269.

[22] Arnold, G., Salt, G., Steven, D., Werkmeister, S., Alabaster, D., & Vanblerk, G. (2009). Compliance testing using the Falling Weight Deflectometer for pavement construction, rehabilitation and area-wide treatments (NZ Transport Agency research report 381). New Zealand Transport Agency.

[23] Bitumen Business Group. (1998). BISAR 3.0 User Manual.

[24] Bureau of location and design. (2018b, 8 March). Evaluation of pavement strength with falling weight deflectometer for rehabilitation with mechanistic design (In Thai). Department of Rural Roads, Thailand. Retrieved 16 September from https://maintenance.drr.go.th/wp-content/uploads/2019/12/drr-2019-12-26_08-40-07_299845.pdf

[25] Sawangsuriya, A., Siriratanachat, T., Thavorn, D., Yueayong, S., & Haisuk, A. (2022). Structural Performance Analysis and Evaluation of Flexible Pavement (In Thai). Bureau of Road Research and Development.

[26] Meteorological Department. (2022, 8 February). Weather in Thailand Year 2021 (In Thai). Retrieved 23 January from http://climate.tmd.go.th/content/file/2355

[27] 911 Metallurgist. (2013, 19 June). List Table of Specific Gravity of Minerals. Retrieved 7 November from https://www.911metallurgist.com/blog/list-table-of-specific-gravity-of-minerals

[28] Department of Civil Engineering. (2022, 18 June). Specific gravity of soil (In Thai). Geotechnical Engineering Research and Development Center. Retrieved 7 November from https://www.gerd.eng.ku.ac.th/Cai/Ch05/ch053_theory.htm

[29] Nampich, S., Kererat, C., Ruayruay, E., Pondsiwasathit, S., Piyapipat, S., Sutasit, W., & Kampliew, S. (2006). Soil Mechanics Laboratory (In Thai). The Thailand Research Fund (TRF).

[30] ASTM International. (2020). ASTM D5858-96 Standard Guide for Calculating In Situ Equivalent Elastic Moduli of Pavement Materials Using Layered Elastic Theory. West Conshohocken, PA.